Materials Horizons

ROYAL SOCIETY OF CHEMISTRY

COMMUNICATION

View Article Online
View Journal | View Issue

Cite this: *Mater. Horiz.*, 2023, **10**, 5016

Received 28th June 2023,
Accepted 11th August 2023

DOI: 10.1039/d3mh00981e

rsc.li/materials-horizons

Two-step fabrication of COF membranes for efficient carbon capture†

Yuhan Wang,‡[ad] Junyi Zhao,‡[bc] Sui Zhang,[c] Zhiming Zhang,[bc] Ziting Zhu,[ad] Meidi Wang,[a] Bohui Lyu,[bc] Guangwei He,[ad] Fusheng Pan*[ad] and Zhongyi Jiang*[abd]

Covalent organic framework (COF) materials have been considered as disruptive membrane materials for gas separation. The dominant one-step method for COF nanosheet synthesis often suffers from coupling among polymerization, assembly and crystallization processes. Herein, we propose a two-step method comprising a framework assembly step and functional group switching step to synthesize COF nanosheets and the corresponding COF membranes. In the first step, the pristine COF-316 nanosheets bearing cyano groups are prepared *via* interfacial polymerization. In the second step, the cyano groups in COF-316 nanosheets were switched into amidoxime groups or carboxyl groups. Through the vacuum-assisted self-assembly method, the COF nanosheets were fabricated into membranes with a thickness below 100 nm. Featuring numerous mass transport channels and homogeneous distribution of functional groups, the amidoxime-modified COF-316 membrane demonstrated excellent separation performance, with a permeance above 500 GPU and a CO_2/N_2 selectivity above 50. The two-step method may inspire the rational design and fabrication of organic framework membranes.

New concepts

Covalent organic framework (COF) materials have been recognized as disruptive membrane materials for carbon capture. The dominant one-step method for COF nanosheet synthesis features the simplicity of operation, but often suffers from the lack of sufficient free functional groups and coupling among polymerization, assembly and crystallization processes. A two-step method comprising a framework assembly step and functional group switching step to synthesize COF nanosheets is proposed in this work. The new concept decouples the construction of a bulk framework and the incorporation of free functional units, conducive to the precise control of COF nanosheet synthesis and thus COF membranes. Herein, functionalized COF-316 membranes were fabricated *via* the two-step method and demonstrated excellent separation performance. Our two-step method shows good universality and affords a platform to design COF and many other organic framework materials for diverse applications.

Introduction

Covalent organic framework (COF) materials featuring an ordered pore structure and tailored chemical functionality exhibit unique separation properties and have been deemed as a disruptive membrane material.[1–5] COFs provide a platform to customize functional groups uniformly distributed within the channels, thus enabling efficient molecular mass transport and separation.[6,7] Nowadays, the functionalization of COFs focuses on the one-step method, where the functional groups are pre-substituted on the monomers followed by the

Zhongyi Jiang

Materials Horizons, as the flagship journal of the RSC in materials science, has gained an excellent reputation over the last ten years. Many innovative studies and new concepts have been published from new material development to frontier applications, endowing this journal wide attention and high citations. I'm honored to be a scientific editor of Materials Horizons and contribute to the sustained development of the journal. Happy 10th anniversary to Materials Horizons.

[a] *Key Laboratory for Green Chemical Technology of Ministry of Education, School of Chemical Engineering and Technology, Tianjin University, Tianjin 300072, China. E-mail: fspan@tju.edu.cn, zhyjiang@tju.edu.cn*
[b] *Joint School of National University of Singapore and Tianjin University, International Campus of Tianjin University Binhai New City, Fuzhou 350207, China*
[c] *Department of Chemical and Biomolecular Engineering, National University of Singapore, Singapore 117585, Singapore*
[d] *Haihe Laboratory of Sustainable Chemical Transformations, Tianjin 300192, China*

† Electronic supplementary information (ESI) available. See DOI: https://doi.org/10.1039/d3mh00981e

‡ These authors contributed equally to this work.

polymerization reaction to assemble the framework.[8,9] The one-step method features simplicity of operation[10] but suffers from a lack of sufficient free functional groups and the coupling of the polymerization, assembly and crystallization processes.[11]

Quite recently, two-step or multi-step construction of COFs has been explored. Zhao's group explored a two-step procedure of COF-to-COF transformation.[12] Addressing the low-crystallinity problem of an azo-linked COF *via* a one-step method, a reversible imine-linked COF was prepared as the template and then *in situ* linker exchange achieved the transformation of the azo-linked COF with high crystallinity. Besides optimizing the linkage, the two-step procedure has the potential to enhance the application performance arising from functional group switching.[13–15] For carbon capture application, the basic groups are often employed as facilitated transport carriers. However, in most cases, the basic groups participate in the COF bulk framework formation and eventually become imine bonds,[16] or amide bonds.[17,18] It can be thus envisioned that if the functional basic groups are incorporated after the framework formation, the basic groups can be retained in the free form.[19]

Herein, we explored a two-step method instead of the one-step method to synthesize COF-316 nanosheets and then assemble these nanosheets into COF-316 membranes. In the first step, the pristine COF-316 nanosheets bearing cyano groups were synthesized based on the irreversible nucleophilic aromatic substitution reaction *via* interfacial polymerization. In the second step, the cyano groups were switched into amidoxime groups or carboxyl groups.[20] The amidoxime-functionalized COF-316 membrane exhibited superior separation performance, with a permeance above 500 GPU and a CO_2/N_2 selectivity above 50. The two-step method demonstrates good universality.

Results and discussion

COF-316 is a dioxin-linked COF material constructed *via* irreversible reactions, with tetrafluorophthalonitrile (TFPN) and 2,3,6,7,10,11-hexahydroxytriphenylene (HHTP) as linear and triangular linkers.[21,22] Different from most COF materials synthesized by reversible reactions, such as the Schiff base reaction, the irreversible nucleophilic aromatic substitution reaction is seriously affected by the adjacent functional groups on the benzene ring. The strong electron withdrawing cyano group is the key to enhancing the electrophilicity of the C–F bond of TFPN and thus endowing the reactivity with HHTP. The cyano group is indispensable in the assembly of the framework; however, the affinity of cyano groups toward CO_2 gas is significantly lower than that of amidoxime or carboxyl groups.[23] Therefore, we further switched cyano groups of COF-316 into amidoxime or carboxy groups.

Considering the inherent limitation in the one-step method, only soluble oligomers were obtained instead of the expected COF. In this study, two-step method was explored to fabricate the functionalized COF-316 *via* combining framework assembly step and functional group switching step. Among the reported COF materials, COF-316 exhibited the following two advantages: (i) ultra-stable bulk framework assembled based on irreversible reactions, ensuring the chemical and structural stability for the second step; (ii) modifiable cyano groups anchored on the pore surface. For CO_2 separation, two functionalities, carboxyl and amidoxime groups could be easily modified on the pore surface by cyano hydrolysis in concentrated NaOH and nucleophilic attack hydroxylamine, respectively.[24]

In the first step of framework assembly, in the previous article, COF-316 was prepared *via* a thermal-solvent method with triethylamine as the catalyst and COF-316 grew into rod-like particles (Fig. S1, ESI†). In this work, COF-316 was synthesized *via* the modified interfacial synthesis and COF-316 nanosheets bearing cyano groups were obtained, deemed as COF-316-CN. The two monomers were each placed in the oil–water phases, and in the middle was separated by a nanofiltration membrane, providing a controlled growth environment and slower monomer diffusion rate (Fig. S2, ESI†).[25] During the reaction process, a layer of amorphous complexes formed on the membrane (Fig. S3, ESI†) and the crystalline nanosheets formed in the aqueous phase. As shown in Fig. 1b, the peaks at 1292 cm^{-1} and 1016 cm^{-1} indicated the characteristic dioxin C–O asymmetric and symmetric stretching modes, representing the formation of the framework.

As shown in Fig. 1e and Fig. S4 (ESI†), COF-316-CN nanosheets displayed an average lateral size of 3–5 μm and an average height of 4 nm, equivalent to a stack of 8–10 atomic layers. The XRD characteristic peaks of COF-316-CN powders were at 4.5°, 9.0° and 24.5° corresponding to (100), (200), and (001) reflection planes in both stacking modes while the peak intensity of the nanosheet was obviously weakened due to only a few layers of stacking (Fig. 1d). The crystallinity of COF-316-CN nanosheets was further confirmed through the orderly arranged lattice fringe and diffraction pots in selected area electron diffraction (SAED) image (Fig. 1e).

In the second step of functional group switching, pristine cyano groups were switched into carboxyl and amidoxime groups, deemed as COF-316-COOH and COF-316-AO. The chemical properties and functional group switching are shown in Fig. 1c. The peaks at 1714 cm^{-1} and the peaks at 923 cm^{-1} indicated the switching of the carboxyl group while the peaks at 3480 cm^{-1}, 3360 cm^{-1} and 3170 cm^{-1} indicated the switching of the amidoxime group. It is worth noting that, the peaks of the cyano group were not observed in COF-316-COOH and COF-316-AO, indicating the complete conversion of the group. As shown in the Fig. 1f, 1g and Fig. S5a (ESI†) the COF-316-COOH and COF-316-AO inherited the crystallinity of parent COF-316-CN, according to the XRD patterns and an orderly arranged lattice fringe in SAED images. The electrostatic potential maps of COF-316-CN, COF-316-COOH and COF-316-AO were analyzed *via* simulation (Fig. 2a–c). The blue regions of N and O in the maps were related to the chemically active sites and the red region of H was related to hydrogen bonding sites. Compared with the pristine COF-316-CN, both the intensity of single anchor site and the density of distribution were both significantly increased in COF-316-COOH and COF-316-AO. With the switching

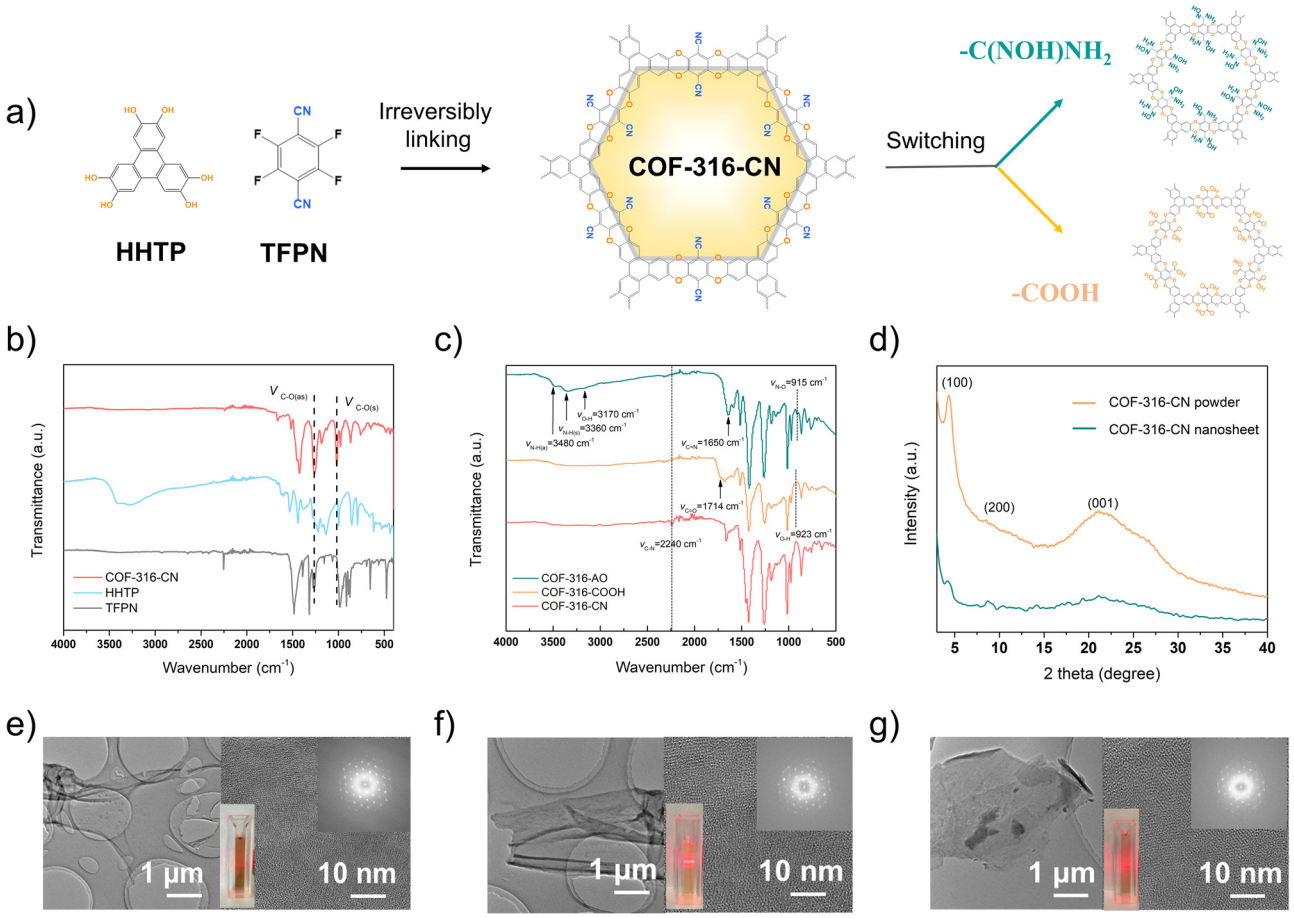

Fig. 1 (a) The schematic diagram of the two step method to fabricate functionalized COF. (b) FT-IR spectra of HHTP, TFPN and COF-316-CN. (c) FT-IR spectra of pristine COF-316-CN, COF-316-COOH and COF-316-AO. (d) XRD pattern of pristine COF-316-CN powder and nanosheet. The TEM, HRTEM images and corresponding selected area electron diffraction patterns (inset) of pristine COF-316-CN (e), COF-316-COOH (f), and COF-316-AO (g).

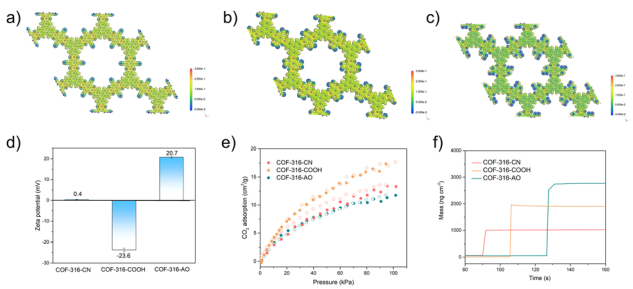

Fig. 2 The electrostatic potential maps of COF-316-CN (a), COF-316-COOH (b), and COF-316-AO (c). The zeta potential analysis (d), CO_2 adsorption behavior (e) and analysis of water-capture ability *via* QCM (f) of pristine COF-316-CN, COF-316-COOH, and COF-316-AO.

of the functional group, the charge characteristics of the pore surface changed simultaneously. The pristine COF-316-CN nanosheets were electrically neutral, with a zeta potential of 0.4 mV while COF-316-COOH nanosheets were electro-negative with a zeta potential of −23.6 mV. COF-316-AO nanosheets displayed electro-positivity, with a zeta potential of 20.7 mV. The thermal properties of COF materials were evaluated *via* thermogravimetric (TG) analysis (Fig. S5b, ESI†). Three TG curves of COF materials followed a similar thermal change process. Within 100–200 °C, the mass loss was related to the release of solvent molecules adsorbed in the pores. Within 200–450 °C, the organic components of the framework continuously decomposed.

The pore characteristics of COF materials were evaluated by CO_2 adsorption and simulation. Before the adsorption test, COF materials were immersed in methylene chloride and vacuum treated for the removal of guests. At 298 K, the CO_2 adsorption of COF-316-CN, COF-316-COOH and COF-316-AO were 13, 17, 12 in $cm^3\ g^{-1}$, respectively. The enthalpy of adsorption was calculated based on GCMC simulation, with $-19.9\ kJ\ mol^{-1}$ (COF-316-CN), $-25.0\ kJ\ mol^{-1}$ (COF-316-COOH) and $-29.6\ kJ\ mol^{-1}$ (COF-316-AO), respectively. In contrast, the improvement of gas uptake within COF-316-COOH was due to stronger interactions, while the decline of gas uptake within COF-316-AO was caused by the smaller pore size and thus space steric effect. The optimized adsorption location and orientation of CO_2 were also investigated. As shown in Fig. S6 (ESI†), within pristine COF-316-CN, cyano group is inert and O of CO_2 mainly interacts with H of the benzene ring, at a distance of 0.32 nm. Within COF-316-COOH and COF-316-AO, the O of CO_2 mainly interacts with H of carboxyl and amidoxime groups with the

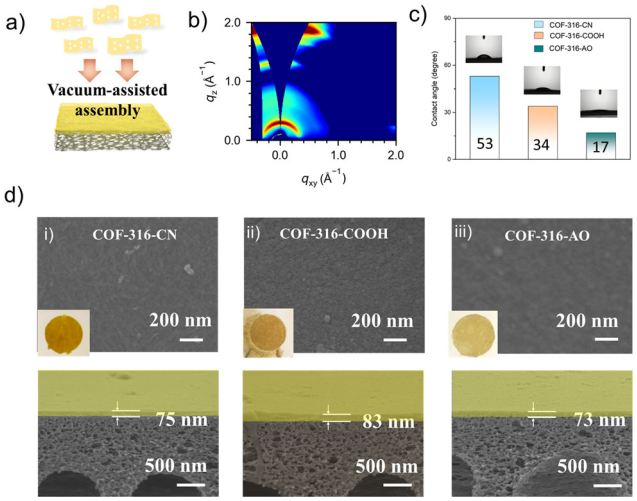

Fig. 3 (a) The schematic diagram of constructing COF membranes. (b) The GIWAX analysis of COF-316-CN membrane. (c) The water contact angle analysis. (d) The SEM images of COF-316-CN membranes, COF-316-COOH membranes, and COF-316-AO membranes from the top-view and the section-view.

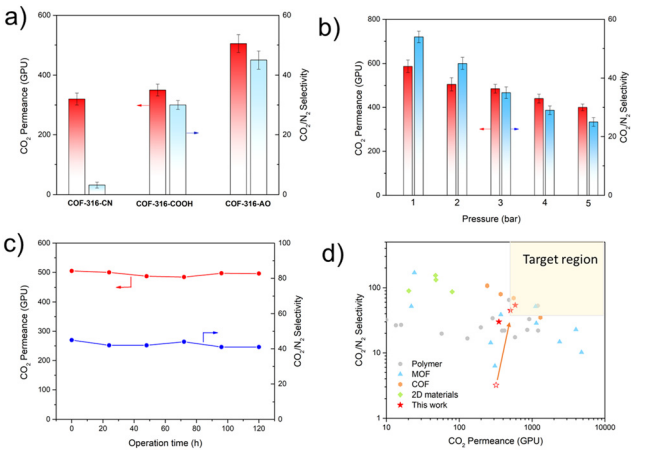

Fig. 4 Separation performances of membranes. (a) CO_2/N_2 (20/80 vol%) mixed-gas separation performances of COF membranes at 100% relative humidity, 298 K and 2 bar. (b) The performance of COF-316-AO under feed gas pressure of 1–5 bar. (c) Long-term test of COF-316-AO membrane tested at 2 bar and 100% relative humidity. (d) Comparison of the CO_2/N_2 separation performances of the membranes and representative membranes in the literature. The light-yellow region is the target area for post-combustion capture of CO_2.[29,30] The data were obtained from the previous literature listed in Table S1 (ESI†).

distance of 0.28 nm and 0.25 nm, respectively. Besides CO_2 adsorption, the water capacity of COF materials was also evaluated *via* the quartz crystal microbalance (QCM). Among the three COF materials, COF-316-AO demonstrated outstanding water-capture ability with the nearly twice the amount of water capacity and higher capture rate.

The COF membrane was fabricated by the vacuum-assisted self-assembly methods at 40 kPa.[26] The loading of the nanosheet was controlled in the range of 0.05 mg cm^{-2} on the polyacrylonitrile (PAN) substrates (pore size of 20–50 nm). As shown in Fig. 3d, the COF-316-CN nanosheets regularly packed and formed a defect-free membrane, with the thickness of nearly 80 nm. As shown in Fig. S7 (ESI†), the membranes inherited the characteristic peaks of their nanosheets and the peaks at 2240 cm^{-1} refer to the PAN substrate. The assembly behavior of the nanosheet was evaluated by the wide-angle X-ray scattering (GIWAXS) experiments (Fig. 3b). The membranes verified the consistent orientation of nanosheets within the COF membranes, of which the Bragg diffraction (100) peak corresponding to the channels emerged at around $q_z = 0$ and relatively weakly presented at $q_{xy} = 0$. The phenomenon indicated the π–π stacking of nanosheet along the *c*-axis and thus formed the one-dimensional channel perpendicular to the PAN substrate. The surface properties of the membrane are indicated by the experiments of water contact angle (Fig. 3c). The pristine COF-316-CN exhibited weak hydrophilicity with the angle of 53°; meanwhile, a significant enhancement of hydrophilicity was achieved with the angles of 34° (COF-316-COOH) and 17° (COF-316-AO). The phenomenon indicated that functionalized groups and water molecules could form more hydrogen bonds, and thus stronger hydrophilicity.[27] Functional group switching of COF-316 membrane was achieved *via* assembly of functional COF nanosheets, not post-modified COF-316 membranes. On the one hand, the substrate cannot endure harsh post-modification conditions. On the other hand, it is hard to precisely control the proportion and position of functional groups by post-modification of membranes.[28]

The separation performance of COF membrane was evaluated based on the WK-method, with a humid feed of CO_2/N_2 mixed gas (20 vol%/80 vol%). As shown in Fig. 4a, the pristine COF-316-CN membrane showed the CO_2 permeance of nearly 300 GPU and CO_2/N_2 selectivity of 3 while COF-316-COOH showed the CO_2 permeance of nearly 400 GPU and CO_2/N_2 selectivity of 30 and COF-316-AO showed the CO_2 permeance of nearly 500 GPU and CO_2/N_2 selectivity of 45. In contrast, COF-316-AO demonstrated the best separation performance, due to the high density of affinity sites and strong interaction with H_2O and CO_2. The pressure effect on the separation performance of COF-316-AO was also investigated. With the absolute pressure of feed increase from 1 bar to 5 bar, the CO_2 permeance decreased from nearly 600 GPU to 400 GPU and the selectivity decreased from 54 to 25. The performance changes complied with the previously reported facilitated transport membranes, which lack adequate carriers to participate in the CO_2 transport under higher pressure.[31,32] Meanwhile, a long-term gas permeation measurement of COF-316-AO membrane was carried out to evaluate the stability. After 100 h, the membrane still could maintain high separation performance, with the permeance of 500 GPU and the selectivity above 40. The separation performance exceeded most CO_2 separation membranes and displayed good application prospects.[1,33]

The CO_2 mass transport mechanism was also investigated. The ideal behaviour of the CO_2 diffusion process through the COF channels was simulated (Fig. S8, ESI†). Within 500 ps, compared with COF-316-CN, fewer CO_2 molecules passed

through the channels of COF-316-AO and more CO_2 molecules passed through the channels of COF-316-COOH. It is worth noting that a large amount of CO_2 was confined in the pores of COF-316-AO. The strong interaction and reduced pore size inhibited the diffusion of molecules, leading to the contribution of physical mechanism to CO_2 diffusion being very limited.[34] During the actual separation process of the humid feed, water would condense within the channel, providing a continuous water environment.[7] In this case, facilitated transport process should be the main contribution to the high performance of COF-316-AO membrane.[35] Within the three COF materials, COF-316-AO embodied the strongest affinity with water and provided the basic microenvironment, in which CO_2 could reversibly convert in the form of $HCO3^-$ in the presence of amidoxime. The chemical properties of the membrane before and after separation were characterized by IR and XPS (Fig. S9 and S10, ESI†), and no obvious new bonds were formed, indicating that the process was a reversible process without irreversible damage to the membrane structure.

The universality of the two-step method was investigated, which was applied to COF-318[21] and TpDb,[36] two COF materials with the cyano group, (Fig. S11, S12 and S13, ESI†). COF-318 shared a similar structure with COF-316, in which the HHTP and 2,3,5,6-tetrafluoro-4-pyridinecarbonitrile (TFPC) were linked by 1,4-dioxin linkages to form crystalline 2D covalent organic frameworks. The FT-IR spectra showed the framework assembly and the switching to amidoxime groups. The XRD pattern showed COF-318 could endure alkaline conditions, retaining crystallinity and frame stability in the second step. On the other hand, TpDb is also deemed as a remarkable chemically stable COF material. For the first step, the framework was assembled, combining the reversible Schiff base reactions and an irreversible enol-to-keto tautomerization. The pristine TpDb showed high crystallinity and characteristic peaks, while the ordered structure was disrupted after switching to amidoxime groups under alkaline conditions. The above results further illustrate that strong bonding structures and stable bulk frameworks are the basis for the follow-up functional group switching.

For more application-oriented scenarios, we explored the universality of preparing COF membranes on different substrates. Besides the vacuum-assisted self-assembly method described above, the hot drop coating method could be used for the preparation of COF-316-AO membranes on inorganic substrates, including AAO substrates, alumina substrates and ITO glass substrates. The membranes were prepared *via* dipping the dispersion on a hot substrate and then slowly volatilizing the solvent. As shown in Fig. S14 (ESI†), the COF-316-AO nanosheets were densely coated on three substrates and formed defect-free membranes.

Conclusions

In summary, we proposed a two-step method to synthesize functionalized COF nanosheets by decoupling the framework assembly process and functional group switching process. Considering the stability of the bulk framework and switchable cyano groups, COF-316 was selected as a showcase and two functionalized COF-316-COOH and COF-316-AO nanosheets were synthesized *via* interface diffusion assembly followed by the switching of cyano groups. The COF nanosheets were then fabricated into COF membranes with a thickness below 100 nm. Combining abundant channels and evenly distributed functional groups, the COF-316-AO membrane exhibited excellent separation performance, with a permeance above 500 GPU and a CO_2/N_2 selectivity above 50. The two-step method was also used for the synthesis of COF-318 and TpDb. Our study may provide some inspirations to design COF and many other organic framework materials for chemical separation and catalysis.

Author contributions

Zhongyi Jiang conceived the article. Yuhan Wang and Junyi Zhao collected the data and wrote the original draft. Zhiming Zhang, Ziting Zhu, and Bohui Lyu simulated the material structure and adsorption behavior. Meidi Wang contributed to data visualization. Sui Zhang and Guangwei He discussed the content. Zhongyi Jiang and Fusheng Pan contributed to the writing – review and editing.

Conflicts of interest

There are no conflicts to declare.

Acknowledgements

The authors gratefully acknowledge financial support from the National Key Research and Development Program of China (No. 2021YFB3802200) and the National Natural Science Foundation of China (No. U20B2023), the Haihe Laboratory of Sustainable Chemical Transformations.

References

1 A. Knebel and J. Caro, *Nat. Nanotechnol.*, 2022, **17**, 911–923.
2 H. J. Wang, M. D. Wang, X. Liang, J. Q. Yuan, H. Yang, S. Y. Wang, Y. X. Ren, H. Wu, F. S. Pan and Z. Y. Jiang, *Chem. Soc. Rev.*, 2021, **50**, 5468–5516.
3 C. S. Diercks and O. M. Yaghi, *Science*, 2017, **355**, eaal1585.
4 S. Y. Ding and W. Wang, *Chem. Soc. Rev.*, 2013, **42**, 548–568.
5 C. Y. Lin, D. T. Zhang, Z. H. Zhao and Z. H. Xia, *Adv. Mater.*, 2018, **30**, 1703646.
6 N. Huang, X. Chen, R. Krishna and D. L. Jiang, *Angew. Chem., Int. Ed.*, 2015, **54**, 2986–2990.
7 H. W. Fan, A. Mundstock, A. Feldhoff, A. Knebel, J. H. Gu, H. Meng and J. Caro, *J. Am. Chem. Soc.*, 2018, **140**, 10094–10098.
8 F. Q. Chen, X. Y. Guan, H. Li, J. H. Ding, L. K. Zhu, B. Tang, V. Valtchev, Y. S. Yan, S. L. Qiu and Q. R. Fang, *Angew. Chem., Int. Ed.*, 2021, **60**, 22230–22235.

9 Z. Dong, C. Zhang, H. Peng, J. Gong, H. Wang, Q. Zhao and J. Yuan, *Mater. Horiz.*, 2020, **7**, 2683–2689.
10 Y. Yang, L. Yang, F. Yang, W. Bai, X. Zhang, H. Li, G. Duan, Y. Xu and Y. Li, *Mater. Horiz.*, 2023, **10**, 268–276.
11 X. Wu, X. Han, Y. Liu, Y. Liu and Y. Cui, *J. Am. Chem. Soc.*, 2018, **140**, 16124–16133.
12 Z. B. Zhou, P. J. Tian, J. Yao, Y. Lu, Q. Y. Qi and X. Zhao, *Nat. Commun.*, 2022, **13**, 2180.
13 Q. P. Zhang, Y. L. Sun, G. Cheng, Z. Wang, H. Ma, S. Y. Ding, B. Tan, J. H. Bu and C. Zhang, *Chem. Eng. J.*, 2020, **391**, 123471.
14 Z. Mi, T. Zhou, W. J. Weng, J. Unruangsri, K. Hu, W. L. Yang, C. C. Wang, K. A. I. Zhang and J. Guo, *Angew. Chem., Int. Ed.*, 2021, **60**, 9642–9649.
15 Y. Yang, L. Yu, T. Chu, H. Niu, J. Wang and Y. Cai, *Nat. Commun.*, 2022, **13**, 2615.
16 Z. Zhang, X. Dong, J. Yin, Z. G. Li, X. Li, D. Zhang, T. Pan, Q. Lei, X. Liu, Y. Xie, F. Shui, J. Li, M. Yi, J. Yuan, Z. You, L. Zhang, J. Chang, H. Zhang, W. Li, Q. Fang, B. Li, X. H. Bu and Y. Han, *J. Am. Chem. Soc.*, 2022, **144**, 6821–6829.
17 D. Stewart, D. Antypov, M. S. Dyer, M. J. Pitcher, A. P. Katsoulidis, P. A. Chater, F. Blanc and M. J. Rosseinsky, *Nat. Commun.*, 2017, **8**, 1102.
18 Y. Lu, Z. B. Zhou, Q. Y. Qi, J. Yao and X. Zhao, *ACS Appl. Mater. Interfaces*, 2022, **14**, 37019–37027.
19 N. Huang, P. Wang and D. Jiang, *Nat. Rev. Mater.*, 2016, **1**, 16068.
20 Z. Li, R. Zhu, P. Zhang, M. Yang, R. Zhao, Y. Wang, X. Dai and W. Liu, *Chem. Eng. J.*, 2022, **434**, 134623.
21 B. Zhang, M. F. Wei, H. Y. Mao, X. K. Pei, S. A. Alshmimri, J. A. Reimer and O. M. Yaghi, *J. Am. Chem. Soc.*, 2018, **140**, 12715–12719.
22 X. Y. Guan, H. Li, Y. C. Ma, M. Xue, Q. R. Fang, Y. S. Yan, V. Valtchev and S. L. Qiu, *Nat. Chem.*, 2019, **11**, 587–594.
23 X. L. Chen, L. Wu, H. M. Yang, Y. Qin, X. H. Ma and N. W. Li, *Angew. Chem., Int. Ed.*, 2021, **60**, 17875–17880.
24 R. Zhu, P. Zhang, X. Zhang, M. Yang, R. Zhao, W. Liu and Z. Li, *J. Hazard. Mater.*, 2022, **424**, 127301.
25 H. Wang, L. Chen, H. Yang, M. Wang, L. Yang, H. Du, C. Cao, Y. Ren, Y. Wu, F. Pan and Z. Jiang, *J. Mater. Chem. A*, 2019, **7**, 20317–20324.
26 M. Wang, P. Zhang, X. Liang, J. Zhao, Y. Liu, Y. Cao, H. Wang, Y. Chen, Z. Zhang, F. Pan, Z. Zhang and Z. Jiang, *Nat. Sustainable*, 2022, **5**, 518–526.
27 A. Ghahari, H. Raissi, S. Pasban and F. Farzad, *npj Clean Water*, 2022, **5**, 28.
28 H. Zeng, S. He, S. S. Hosseini, B. Zhu and L. Shao, *Adv. Membr.*, 2022, **2**, 100015.
29 Y. Wang, H. Jiang, Z. Guo, H. Ma, S. Wang, H. Wang, S. Song, J. Zhang, Y. Yin, H. Wu, Z. Jiang and M. D. Guiver, *Energy Environ. Sci.*, 2023, **16**, 53–75.
30 L. M. Robeson, *J. Membr. Sci.*, 2008, **320**, 390–400.
31 S. F. Wang, X. Q. Li, H. Wu, Z. Z. Tian, Q. P. Xin, G. W. He, D. D. Peng, S. L. Chen, Y. Yin, Z. Y. Jiang and M. D. Guiver, *Energy Environ. Sci.*, 2016, **9**, 1863–1890.
32 C. Y. Chuah, K. Goh, Y. Q. Yang, H. Q. Gong, W. Li, H. E. Karahan, M. D. Guiver, R. Wang and T. H. Bae, *Chem. Rev.*, 2018, **118**, 8655–8769.
33 T. Zhu, J. Dong, H. Liu and Y. Wang, *Mater. Horiz.*, 2023, **10**, 3024–3033.
34 A. Sharma, A. Malani, N. V. Medhekar and R. Babarao, *CrystEngComm*, 2017, **19**, 6950–6963.
35 L. Xiang, D. Liu, H. Jin, L.-W. Xu, C. Wang, S. Xu, Y. Pan and Y. Li, *Mater. Horiz.*, 2020, **7**, 223–228.
36 Q. Sun, B. Aguila, L. D. Earl, C. W. Abney, L. Wojtas, P. K. Thallapally and S. Q. Ma, *Adv. Mater.*, 2018, **30**, 1705479.